2018 7th IEEE International Conference on Biomedical
Robotics and Biomechatronics (Biorob)
Enschede, The Netherlands, August 26-29, 2018

Markovian robust compliance control based on electromyographic signals*

Andres L. Jutinico[2], Felix M. Escalante[1], Jonathan C. Jaimes[2], Marco H. Terra[1] and Adriano A. G. Siqueira[2]

Abstract— **In this paper, we deal with the human-robot interaction control problem. Levels of actuation of the user are considered in the human-robot interaction model from a stochastic point of view. It is given in terms of a Markovian approach. Electromyographic signals are used to compute jump parameters between different levels of interaction. In this way, human neuromuscular system defines the behavior of the Markov chain. A unified approach composed by robust Kalman filter and robust regulator for discrete-time Markovian jump linear systems is proposed. Also, a serious game is used to generate visual feedback and promote the active participation of the user. Experimental results show high accuracy in the Markovian compliance control for a robotic platform applied in ankle rehabilitation.**

I. INTRODUCTION

Rehabilitation Robotics (RR) is a research area where interactive robots are used to recover motor functions of people with neurological injuries [1], [2], [3]. In this context, several interaction control approaches have been considered to deal with Human-Robot Interaction (HRI) problems [4], [5], [6]. However, when it is considered the interaction between robot and patient, different neuromuscular responses can be evidenced according to the injury degree. We have advocated that the identification of the human participation should be taken into account in the development of interaction controls [7]. In [8], we presented a control strategy for robotic rehabilitation that regards temporal transitions of the human impedance around the joints. Such transitions were modeled via discrete-time Markov chain, considering a set of operation modes, a probability matrix, and the jump parameter. However, the method used to identify jumps between modes, based only on kinematic data, does not take into account the neuromuscular activity of the user. Therefore, we propose to use the electromyographic signals for on-line detection of the jump parameter.

We solve this human-robot interaction control problem based on a unified approach of the Robust Kalman Filter [9], [10] and the Robust Regulator [11] for Discrete-time Markovian jump Linear Systems (RKF and RR-DMJLS, respectively). Simulation results are shown in [12]. A robotic rehabilitation scenario is proposed, where a series elastic actuator (SEA)-based Robotic Platform for Ankle Rehabilitation (SRPAR), and an interactive game for therapy (serious game) are used. We are motivated to apply robust advanced control and filtering approaches for lower limb rehabilitation therapy for several reasons. First, to provide a Markovian compliance control that takes into account abrupt changes in the parameters of the dynamic systems, intrinsic characteristic of HRI systems. Second, to improve the online estimation methodology of the jump parameter, θ_k, proposed in our paper in [7]. For this purpose, the electromyographic (EMG) signal of muscular activities of Peroneus Longus (PL) and Gastrocnemius (GA) muscles are extracted. They participate directly in the plantarflexion and dorsiflexion movements of the ankle. Third, we are interested in validating our proposal in individuals with stroke in a future work. Therefore, safety and precision are crucial factors in these preliminary results.

The rest of this paper is organized as follows. Section II presents the experimental setup and the SRPAR nominal model. Section III and IV address the control strategies used for controlling the SRPAR in interaction with the human being. Sections V and VI report the experimental protocol and results to illustrate the effectiveness of the methods. Finally, Section VII provides the conclusions and some final remarks for future work.

II. EXPERIMENTAL SETUP AND NOMINAL MODEL

A. Experimental Setup

The experimental setup is composed of the SRPAR, the electromyographic system, and the serious game, as shown in Fig. 1. This setup provides controlled assistance during dorsiflexion and plantarflexion movements. The platform has a series elastic actuator (SEA), an angular position encoder, and a force sensor, where a linear potentiometer measures the spring deformation of the SEA. The SRPAR also counts with power driver *EPOS 24/5*, which regulates current and velocity of the motor. Electromyographic signals of leg muscles are measurements through the *Trigno Wireless Delsys* system. The EMG sensor has the range of 11 mv and resolution of 168 nV/bit. For signal conditioning, an electronic amplifier circuit with a gain equal to 100 is used to send signals to analog to digital converter in the *EPOS 24/5*. The serious game is development in C++ language. It

*This work is supported by Pro-Rectory of Research of University of São Paulo, Coordination for the Improvement of Higher Education Personnel (CAPES), Colciencias (Colombia), Antonio Nariño University-PFAN, National Council for Scientific and Technological Development (CNPq) under grants 132221/2013-6 and 142080/2016-0, and São Paulo Research Foundation (FAPESP) under grants 2011/04074-3 and 2013/14756-0. Also has a partial support of the project INCT-INSac (Nat. Inst. of Science and Technology for Cooperative Autonomous Systems) - under grants CNPq 465755/2014-3, FAPESP 2014/50851-0.

[1] Felix M. Escalante and Marco H. Terra with the Department of Electrical Engineering, University of São Paulo at São Carlos, Brazil (e-mail: maurinho707@usp.br; terra@sc.usp.br).

[2] Andres L. Jutinico, Jonathan C. Jaimes and Adriano A. G. Siqueira with the Department of Mechanical Engineering, University of São Paulo at São Carlos, Brazil (e-mail: {ajutinico, jonathancj}@usp.br; siqueira@sc.usp.br).

978-1-5386-8183-1/18/$31.00 ©2018 IEEE

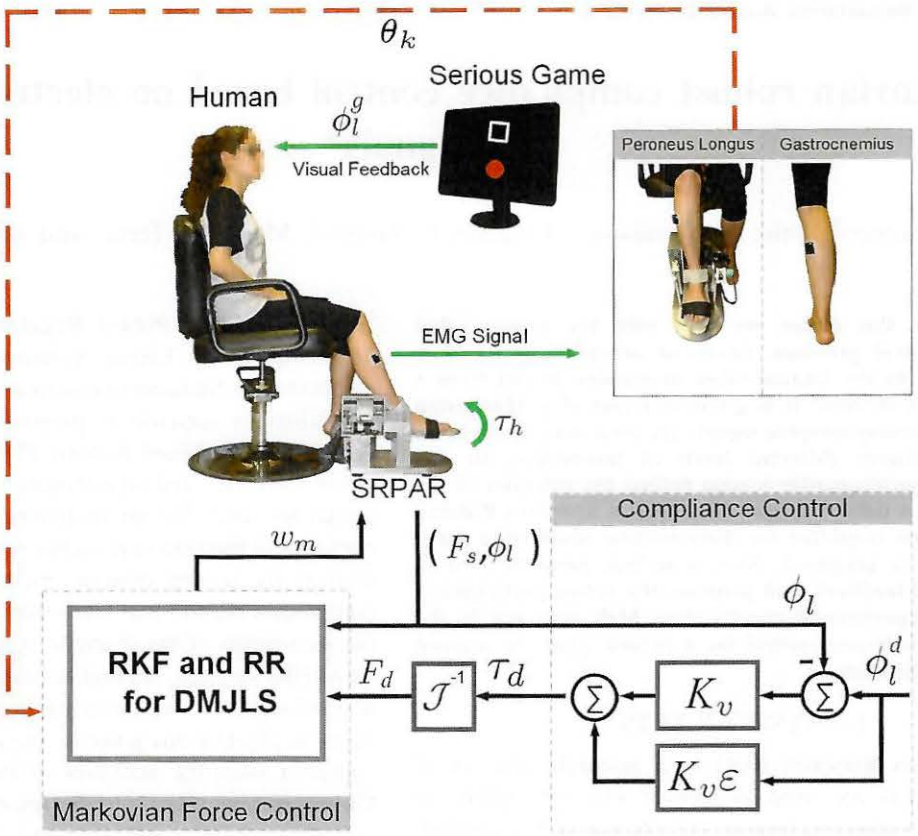

Fig. 1. **Overall scheme for the Human-robot system:** Experimental setup and interaction control.

$$\underbrace{\begin{bmatrix}\ddot{F}_s\\ \dot{F}_s\\ \dot{\phi}_l\end{bmatrix}}_{\dot{x}_a} = \underbrace{\begin{bmatrix}-\frac{C_l}{J_l} & \left(\frac{-K_s}{M_{meq}} - \frac{K_h+K_s\mathcal{J}^2}{J_l}\right) & 0\\ 1 & 0 & 0\\ -(K_s\mathcal{J})^{-1} & 0 & 0\end{bmatrix}}_{F_a} \underbrace{\begin{bmatrix}\dot{F}_s\\ F_s\\ \phi_l\end{bmatrix}}_{x_a} + \underbrace{\begin{bmatrix}\frac{K_s}{\rho N_p}\left(\frac{C_l}{J_l} - \frac{B_{meq}}{M_{meq}}\right) + \frac{\rho N_p K_s C_m}{M_{meq}}\\ 0\\ (\rho N_p\mathcal{J})^{-1}\end{bmatrix}}_{B_a} w_m + \underbrace{\begin{bmatrix}\frac{K_s\mathcal{J}}{J_l}\\ 0\\ 0\end{bmatrix}}_{G_a} \tau_h + \underbrace{\begin{bmatrix}\frac{K_h K_s}{\rho N_p J_l}\\ 0\\ 0\end{bmatrix}}_{G_h} \phi_m, \quad (1)$$

$$y = \underbrace{\begin{bmatrix}0 & 1 & 0\end{bmatrix}}_{C}\begin{bmatrix}\dot{F}_s\\ F_s\\ \phi_l\end{bmatrix} + \underbrace{\begin{bmatrix}1\end{bmatrix}}_{D} v_k. \quad (2)$$

allows feedback visualization, as well as, motivates the user to do movements with a predefined sequence.

B. State-space Model of the SRPAR

The SRPAR dynamics is represented by Equations (1) and (2). Here, the state vector, x_a, is composed by the angular position of the load, ϕ_l, the spring force, F_s, and its first derivate respect to time, $\dot{F}_s$. The angular velocity of the motor, ω_m, is the control input of the system. The human torque, τ_h, and the angular position of the motor, ϕ_m, are considered input disturbances and v_k represents the output noise vector.

The assisted torque provided by the SRPAR is proportional to the spring force, $F_s = K_s\Delta X$, where, K_s and ΔX are the stiffness constant and deformation of the spring. The mechanical impedance of the internal motor-transmission system is compound by a cartesian inertia, $M_{meq} = \rho^2(J_p + N_p^2 J_m)$, and damping, $B_{meq} = \rho^2(C_p + N_p^2 C_m)$; J and C are the torsional inertia and damping with subscripts m for motor and p for the pulley. N_p is the pulley ratio and ρ is a rotational-to-linear factor of ball screw lead.

The output load consists of a 4-link mechanism attached to the foot. The angular movement is mapped to linear displacement by the Jacobian constant $\mathcal{J}$. A second-order model (stiffness, damping, and inertia) was used to represent ankle dynamics. The output mechanical impedance describing the interaction between the ankle and platform is characterized by an equivalent inertia, $J_l = J_{plat} + J_h$, damping, $C_l = C_{plat} + C_h$, and stiffness, K_h, with subscripts $_{plat}$ for platform and $_h$ for human.

The model considers two operation modes: the resistive mode, $\theta_k = 1$, when the platform torque is opposite to foot torque and the passive mode, $\theta_k = 2$, when the platform

carries the user's foot.

The representation of state-space in (1)-(2) is an alternative form of the model presented in [7, eq.(20), eq.(21)]. It is worth mentioning that all parameters of the dynamic model are the same presented in [7, Table I]. The parameters used for each Markovian operation mode (See Table I) are based on [13], and [14].

TABLE I
HUMAN PARAMETERS

Parameter	$\theta_k = 1$	$\theta_k = 2$
$J_h\ (kg \cdot m^2)$	0.08	0.02
$C_h\ (N \cdot m \cdot s/rad)$	5	0.5
$K_h\ (N \cdot m/rad)$	200	20

III. THE COMPLIANCE CONTROL

The compliance control is used to obtain an appropriate interaction between user and robot. It is given by:

$$\tau_d = K_v(\phi_l^d - \phi_l) + K_v \varepsilon \phi_l^d, \tag{3}$$

where τ_d is the desired torque, ϕ_l^d is the desired trajectory for the load, and K_v is the virtual stiffness. Also, it is included a feed-forward term, $K_v \varepsilon \phi_l^d$, for reducing overshooting, where ε is an adjustment term. The interaction control scheme for the human-robot system is shown in Fig. 1. The desired torque, τ_d, is further converted to a desired force, F_d, which is defined as input to the Markovian robust force controller.

IV. FORCE CONTROLLER BASED ON ROBUST KALMAN FILTER AND ROBUST REGULATOR FOR DMJLS

Consider the human-robot model in (1)-(2), which relating the physical parameters of the SRPAR and a simplified model of human ankle joint. To ensure an accurate compliance control, we propose a Markovian robust force controller based on RKF and RR-DMJLS.

Now let us consider the platform and the neuromuscular system modeled like DMJLS subject to parametric uncertainties with partial access to the state variables. Its model includes the state vector $x_k \in \mathbb{R}^n$, the measurement output vector $y_k \in \mathbb{R}^p$, the control input $u_k \in \mathbb{R}^{m_1}$, the disturbance input $w_k \in \mathbb{R}^{m_2}$ and the output noise vector $v_k \in \mathbb{R}^t$:

$$\begin{aligned} x_{k+1} &= (F_{\theta_k,k} + \delta F_{\theta_k,k})x_k + (B_{\theta_k,k} + \delta B_{\theta_k,k})u_k \\ &\quad +(G_{\theta_k,k} + \delta G_{\theta_k,k})w_k, \\ y_k &= C_{\theta_k,k}x_k + D_{\theta_k,k}v_k, \qquad k = 0, ..., \mathcal{N}-1, \end{aligned} \tag{4}$$

where $F_{\theta_k,k} \in \mathbb{R}^{n\times n}$, $B_{\theta_k,k} \in \mathbb{R}^{n\times m_1}$, $G_{\theta_k,k} \in \mathbb{R}^{n\times m_2}$, $C_{\theta_k,k} \in \mathbb{R}^{p\times n}$ and $D_{\theta_k,k} \in \mathbb{R}^{p\times t}$ are nominal parameter matrices. The uncertainty matrices $\delta F_{\theta_k,k} \in \mathbb{R}^{n\times n}$ and $\delta B_{\theta_k,k} \in \mathbb{R}^{n\times m_1}$ are defined from $H_{\theta_k,k} \in \mathbb{R}^{n\times q}$ (nonzero matrix), $E_{F_{\theta_k,k}} \in \mathbb{R}^{l\times n}$, $E_{B_{\theta_k,k}} \in \mathbb{R}^{l\times m_1}$,

$$[\delta F_{\theta_k,k}\ \delta B_{\theta_k,k}] = H_{\theta_k,k}\Delta^1_{\theta_k,k}\begin{bmatrix} E_{F_{\theta_k,k}} & E_{B_{\theta_k,k}} \end{bmatrix}, \tag{5}$$

$\Delta^1_{\theta_k,k} \in \mathbb{R}^{q\times l}$ is an arbitrary matrix such that $\| \Delta^1_{\theta_k,k} \| \leq 1$. Through the use of a discrete-time Markov chain $\{\theta_k\}_{k=0}^{\mathcal{N}-1}$ is possible to model time transitions and operation modes in a process, where θ_k is called the jump parameter and belongs to a finite set $\Theta := \{1, ..., s\}$ and admits values at each time moment k in order to establish the Markovian state and transitions between them. The probability matrix for state transitions of the Markov chain is given by $\mathbb{P} = [p_{i,j}] \in \mathbb{R}^{sxs}$ and its inputs satisfy the following constraints:

$$\begin{aligned} &Prob[\theta_{k+1} = j|\theta_k = i] = p_{ij}, \quad Prob[\theta_0 = i] = \pi_i, \\ &\textstyle\sum_{j=1}^{s} p_{ij} = 1, \quad 0 \leq p_{ij} \leq 1. \end{aligned} \tag{6}$$

A. Robust Regultor for DMJLS

The Robust Regulator for Discrete-Time Markovian Jump Linear Systems reporting in [11] and shown in (8). The inputs for this algorithm are the parameters of the dynamical model (4)-(6), the weighting matrices $P_{c.i,k} \succ 0$, $Q_{c,i,k} \succ 0$, $R_{c,i,k} \succ 0$, and the μ_c parameter. Algorithm outputs are the optimal response of closed-loop system x^*_{k+1}, the control action u^*_k, the control vector $K_{i,k}$, and the closed loop matrix $L_{i,k}$. When there exists full measurement of states and $\mu_c \to +\infty$, therefore $\mathcal{W}_{i,k} \to 0$, the system robustness is guaranteed,

$$\begin{cases} L_{i,k} = F_{i,k} + B_{i,k}K_{i,k} \\ E_{F_{i,k}} + E_{B_{i,k}}K_{i,k} = 0. \end{cases} \tag{7}$$

Robust Regulator for DMJLS
Initial Conditions: Set x_0, θ_0, $\mathbb{P}$, $P_i(N) \succ 0$, $\forall i \in \{1, ..., s\}$.
Step 1: (*Backward*). Calculate for all $k = N-1, \ldots, 0$:

$$\Psi_{c,i,k+1} = \sum_{j=1}^{s} P_{c,j,k+1}p_{ij}$$

$$\begin{bmatrix} L_{i,k} \\ K_{i,k} \\ P_{c.i,k} \end{bmatrix} = \begin{bmatrix} 0 & 0 & 0 & 0 & I & 0 \\ 0 & 0 & 0 & 0 & 0 & I \\ 0 & 0 & -I & \hat{F}^T_{i,k} & 0 & 0 \end{bmatrix}$$

$$\begin{bmatrix} \Psi^{-1}_{c,i,k+1} & 0 & 0 & 0 & I & 0 \\ 0 & R^{-1}_{c,i,k} & 0 & 0 & 0 & I \\ 0 & 0 & Q^{-1}_{c,i,k} & 0 & 0 & 0 \\ 0 & 0 & 0 & \mathcal{W}_{i,k} & \hat{I} & -\hat{B}_{i,k} \\ I & 0 & 0 & \hat{I}^T & 0 & 0 \\ 0 & I & 0 & -\hat{B}^T_{i,k} & 0 & 0 \end{bmatrix}^{-1} \begin{bmatrix} 0 \\ 0 \\ -I \\ \hat{F}_{i,k} \\ 0 \\ 0 \end{bmatrix}$$

$$\mathcal{W}_{i,k} = \begin{bmatrix} \mu_c^{-1}I - \hat{\lambda}^{-1}_{c,i,k}H_{i,k}H^T_{i,k} & 0 \\ 0 & \hat{\lambda}^{-1}_{c,i,k}I \end{bmatrix}, \hat{I} = \begin{bmatrix} I \\ 0 \end{bmatrix},$$

$$\hat{B}_{i,k} = \begin{bmatrix} B_{i,k} \\ E_{B_{i,k}} \end{bmatrix}, \hat{F}_{i,k} = \begin{bmatrix} F_{i,k} \\ E_{F_{i,k}} \end{bmatrix}, \quad \lambda_{i,k} > \| \mu_c H^T_{i,k}H_{i,k} \| .$$

Step 2: (*Forward*). Obtain for each $k = 0, \ldots N-1$:

$$\begin{bmatrix} x^*_{k+1} \\ u^*_k \end{bmatrix} = \begin{bmatrix} L_{\theta_k,k} \\ K_{\theta_k,k} \end{bmatrix} x^*_k. \tag{8}$$

B. Robust Kalman Filter for DMJLS

Let us consider a reduced-order estimator to reconstruct some unmeasured states in (4). Consider also the model in (9) as a partitioned model of (4), where $\bar{x}_k \in \mathbb{R}^{\bar{n}}$ is the state vector to be estimated, $y_k \in \mathbb{R}^p$ is the measurement output vector, $\bar{u}_k \in \mathbb{R}^{\bar{m}_1}$ is the control input, $w_k \in \mathbb{R}^{m_2}$ is the

disturbance input with variance $Q_k \in \mathbb{R}^{\bar{m}_2 \times \bar{m}_2}$ and $v_k \in \mathbb{R}^{\bar{t}}$ is the output noise vector with variance $R_k \in \mathbb{R}^{\bar{t}\times\bar{t}}$.

$$\begin{aligned} \bar{x}_{k+1} &= (\bar{F}_{\theta_k,k} + \delta\bar{F}_{\theta_k,k})\bar{x}_k + (\bar{B}_{\theta_k,k} + \delta\bar{B}_{\theta_k,k})\bar{u}_k \\ &+(\bar{G}_{\theta_k,k} + \delta\bar{G}_{\theta_k,k})w_k, \\ y_k &= \bar{C}_{\theta_k,k}\bar{x}_k + \bar{D}_{\theta_k,k}v_k, \qquad k \geq 0, \end{aligned} \tag{9}$$

the nominal matrices $\bar{F}_{\theta_k,k} \in \mathbb{R}^{\bar{n}\times\bar{n}}$, $\bar{B}_{\theta_k,k} \in \mathbb{R}^{\bar{n}\times\bar{m}_1}$, $\bar{G}_{\theta_k,k} \in \mathbb{R}^{\bar{n}\times\bar{m}_2}$, $\bar{C}_{\theta_k,k} \in \mathbb{R}^{\bar{p}\times\bar{n}}$, $\bar{D}_{\theta_k,k} \in \mathbb{R}^{\bar{p}\times\bar{t}}$ have appropriate dimensions, and the uncertain matrices $\delta\bar{F}_{\theta_k,k} \in \mathbb{R}^{\bar{n}\times\bar{n}}$, $\delta\bar{B}_{\theta_k,k} \in \mathbb{R}^{\bar{n}\times\bar{m}_1}$, $\delta\bar{G}_{\theta_k,k} \in \mathbb{R}^{\bar{n}\times\bar{m}_2}$, $\delta\bar{C}_{\theta_k,k} \in \mathbb{R}^{\bar{p}\times\bar{n}}$, $\delta D_{\theta_k,k} \in \mathbb{R}^{\bar{p}\times\bar{t}}$, are given by

$$\begin{aligned} &\left[\begin{array}{ccc} \delta\bar{F}_{\theta_k,k} & \delta\bar{B}_{\theta_k,k} & \delta\bar{G}_{\theta_k,k} \end{array}\right] = \\ &M_{\theta_k,k}\Delta^1_{\theta_k,k}\left[\begin{array}{ccc} E_{\bar{F}_{\theta_k,k}} & E_{\bar{B}_{\theta_k,k}} & E_{\bar{G}_{\theta_k,k}} \end{array}\right], \| \Delta^1_{\theta_k,k} \| \leq 1. \end{aligned} \tag{10}$$

where, $E_{\bar{F}_{\theta_k,k}}$,$E_{\bar{G}_{\theta_k,k}}$ and $E_{\bar{B}_{\theta_k,k}}$ have appropriate dimensions, $M_{\theta_k,k}$ is non zero matrix, and $\Delta^1_{\theta_k,k}$ is an arbitrary contraction. Assume that $\bar{x}_0$, w_k and v_k are mutually independent zero-mean Gaussian random variables with variances $\mathbb{E}\{\bar{x}_0\bar{x}_0^T\} = \Pi_0 \succ 0$, $\mathbb{E}\{w_0w_0^T\} = Q_k \succ 0$ and $\mathbb{E}\{v_0v_0^T\} = R_k \succ 0$, respectively.

The framework to describe the RKF-DMJLS in the predicted and filtered forms can be seen in (11) and its auxiliary matrices in (12)-(16). To ensure the optimal response, the parameter $\alpha \geq 1$ is selected.

Robust Kalman filter for DMJLS.
Consider (9), with $\Pi_0 \succ 0$, $Q_k \succ 0$, and $R_k \succ 0$.
Initial Conditions: $P_{0|-1} = \Pi_0$ and $\hat{x}_{0|-1} = 0$.
Step $k \geq 0$: Update $\{\hat{x}_{k+1|k}; P_{k+1|k}\}$ and $\{\hat{x}_{k|k}; P_{k|k}\}$.

$$\Psi_{i,k+1|k} = \sum_{j=1}^{s} p_{ij} P_{i,k+1|k},$$

$$\begin{bmatrix} \hat{x}_{k|k} & P_{i,k|k} & * \\ \hat{x}_{k+1|k} & * & P_{i,k+1|k} \end{bmatrix} =$$

$$\begin{bmatrix} 0 \\ 0 \\ 0 \\ I \end{bmatrix}^T \begin{bmatrix} \mathfrak{P}_k & 0 & I & 0 \\ 0 & \mathfrak{S}_k & \mathfrak{A}_k & \mathfrak{B}_k \\ I & \mathfrak{A}_k^T & 0 & 0 \\ 0 & \mathfrak{B}_k^T & 0 & 0 \end{bmatrix}^{-1} \begin{bmatrix} 0 & 0 \\ \mathfrak{Z}_k & 0 \\ 0 & 0 \\ 0 & -I \end{bmatrix},$$

$$\mathfrak{P}_k = \begin{bmatrix} \Psi_{i,k|k-1} & 0 & 0 \\ 0 & Q_k & 0 \\ 0 & 0 & R_k \end{bmatrix}, \mathfrak{S}_k = \begin{bmatrix} \mu^{-1}I & 0 & 0 \\ 0 & \mathcal{W}_{1,i,k} & 0 \\ 0 & 0 & \mathcal{W}_{2,i,k} \end{bmatrix},$$

$$\mathfrak{A}_k = \begin{bmatrix} I & 0 & 0 \\ 0 & \hat{G}_{i,k} & 0 \\ 0 & 0 & \hat{D}_{i,k} \end{bmatrix}, \mathfrak{B}_k = \begin{bmatrix} -I & 0 \\ \hat{F}_{i,k} & -\hat{I} \\ \hat{C}_{i,k} & 0 \end{bmatrix}, \mathfrak{Z}_k = \begin{bmatrix} -\hat{x}_{k|k-1} \\ -\hat{B}_{i,k}\bar{u}_k \\ \mathcal{Y}_k \end{bmatrix}. \tag{11}$$

$$\hat{\lambda}_{i,k} = (1+\alpha)\left\| \begin{matrix} \mu M_{i,k}^T M_{i,k} & 0 \\ 0 & \mu I \end{matrix} \right\|, \tag{12}$$

$$\mathcal{W}_{1,i,k} = \begin{bmatrix} (\mu^{-1}I - \hat{\lambda}_{i,k}^{-1} M_{i,k} M_{i,k}^T) & 0 \\ 0 & \hat{\lambda}_{i,k}^{-1} I \end{bmatrix}, \tag{13}$$

$$\mathcal{W}_{2,i,k} = \begin{bmatrix} (\mu^{-1}I - \hat{\lambda}_{i,k}^{-1} I) & 0 \\ 0 & \hat{\lambda}_{i,k}^{-1} I \end{bmatrix}, \hat{I} = \begin{bmatrix} I \\ 0 \end{bmatrix}, \tag{14}$$

$$\hat{F}_{i.k} = \begin{bmatrix} \bar{F}_{i,k} \\ E_{\bar{F}_{i,k}} \end{bmatrix}, \hat{B}_{i.k} = \begin{bmatrix} \bar{B}_{i,k} \\ E_{\bar{B}_{i,k}} \end{bmatrix}, \mathcal{Y}_k = \begin{bmatrix} y_k \\ 0 \end{bmatrix}. \tag{15}$$

$$\hat{G}_{i,k} = \begin{bmatrix} \bar{G}_{i,k} \\ E_{\bar{G}_{i,k}} \end{bmatrix}, \hat{C}_{i,k} = \begin{bmatrix} \bar{C}_{i,k} \\ 0 \end{bmatrix}, \hat{D}_{i,k} = \begin{bmatrix} \bar{D}_{i,k} \\ 0 \end{bmatrix}. \tag{16}$$

C. Output Feedback Force Control Design

1) Nominal Model : The discrete time model of System (1) is calculated using $F_{a_k} = I + F_a T_s \eta$, $B_{a_k} = \eta T_s B_a$, $G_{a_k} = \eta T_s G_a$ and $G_{b_k} = \eta T_s G_b$, with $\eta = \sum_{k_n=0}^{9} \frac{F_a^{k_n} T_s^{k_n}}{(k_n+1)!}$, and $T_s = 2$ ms. The steady-state force error can be reduce by including an integral action in the nominal model, hence,

$$\underbrace{\begin{bmatrix} x_{a_{k+1}} \\ x_{int_{k+1}} \end{bmatrix}}_{x_{k+1}} = \underbrace{\begin{bmatrix} F_{a_k} & 0 \\ C_a T_s & 1 \end{bmatrix}}_{F_{i,k}} \underbrace{\begin{bmatrix} x_{a_k} \\ x_{int_k} \end{bmatrix}}_{x_k} + \underbrace{\begin{bmatrix} B_{a_k} \\ 0 \end{bmatrix}}_{B_{i,k}} u_k + \underbrace{\begin{bmatrix} 0 \\ T_s \end{bmatrix}}_{Br_{i,k}} F_{d_k} + \underbrace{\begin{bmatrix} G_{a_k} & G_{b_k} \\ 0 & 0 \end{bmatrix}}_{G_{i,k}} \begin{bmatrix} \tau_{h_k} \\ \phi_m \end{bmatrix}, \tag{17}$$

where, $F_{d_k} = \mathcal{J}^{-1}\tau_{d_k}$, is a force desired signal, $C_a = [0\ -1\ 0]$ and $F_{i,k}$, $B_{i,k}$, $G_{i,k}$ are the nominal parametric matrices of the model, according to (4). In Appendix are shown the numerical values of design parameters for the RKF and RR-DMJLS.

2) The Transition Probability Matrix and The Jump Parameter: The transition probability matrix, $\mathbb{P}$, and the jump parameter, θ_k, are defined as follow,

$$\mathbb{P} = \begin{bmatrix} 0.6 & 0.4 \\ 0.4 & 0.6 \end{bmatrix}, \tag{18}$$

$$\theta_k = \begin{cases} 1 & \text{if} \quad \Omega^f_{PLk|k-1} > t_{PL} \\ & \quad \text{or } \Omega^f_{GAk|k-1} > t_{GA}, \\ 2 & \text{otherwise,} \end{cases} \tag{19}$$

for each $k = 0, ..., \mathcal{N}-1$. Variables $\Omega^f_{PLk|k-1}$ and $\Omega^f_{GAk|k-1}$ are filtered measurements of the muscular activities from Peroneus Longus and Gastrocnemius. The variable $\Omega^f_{PLk|k-1}$ is calculating using the nominal Kalman filter,

$$\begin{aligned} x_{PLk+1|k} &= A_f x_{PLk|k-1} + L_f(|\Omega_{PL_k}| - C_f x_{PLk|k-1}), \\ \Omega^f_{PLk|k-1} &= C_f x_{PLk|k-1}, \end{aligned} \tag{20}$$

where Ω_{PL_k} corresponds to the electromyographic measurement of the Peroneus Longus, which is amplified and digitalized. Matrices A_f, L_f and C_f are given by:

$$A_f = \begin{bmatrix} 0.999 & -4\cdot10^{-4} & -2\cdot10^{-5} & -1\cdot10^{-5} \\ 6\cdot10^{-5} & 0.999 & 0 & 0 \\ 0 & 3\cdot10^{-5} & 0.999 & 0 \\ 0 & 0 & 1\cdot10^{-5} & 1 \end{bmatrix}, L_f = \begin{bmatrix} 7.64 \\ 10.1 \\ 2.17 \\ 0.06 \end{bmatrix},$$

$$C_f = [0 \quad 0 \quad 0 \quad 0.084]. \tag{21}$$

Constants t_{PL} and t_{GA} are thresholds defined according to the electromyographic levels of each user. The same method is used to calculate the variable $\Omega^f_{GAk|k-1}$.

3) The Dynamic Controller: Equation (22) shows the control gains given by the RR-DMJLS,

$$K_{\theta_k} = \begin{bmatrix} K_{1,\theta_k} & K_{2,\theta_k} & K_{3,\theta_k} & K_{int,\theta_k} \end{bmatrix},$$

$$K_{1_k} = \begin{bmatrix} -0.0101 & -8.36 & 2.18 & 80.98 \end{bmatrix}, \quad (22)$$

$$K_{2_k} = \begin{bmatrix} -0.0281 & -3.35 & 12.8 & 46.86 \end{bmatrix}.$$

The control law is modified to consider the state estimates by the RKF-DMJLS,

$$u_k = [K_{1,\theta_k}\ K_{2,\theta_k}]\hat{x}_{k|k-1} + K_{3,\theta_k} x_{3_k} + K_{int,\theta_k} x_{int_k}, \quad (23)$$

where $\hat{x}_{k|k-1} = [\hat{x}_{1,k|k-1} \quad \hat{x}_{2,k|k-1}]^T$, are estimates of spring force derivatives, $\dot{F}_s$, and springs force, F_s, respectively. The state x_{3_k} is the angular position of the load, ϕ_l, and x_{int_k} is the integral action defined in (17).

V. Experimental Protocol

In order to check the effectiveness of Markovian compliance control, we performed an experimental protocol. We asked a healthy user to sit comfortably, then the robot was adequately attached to the foot, and electromyographic sensors were situated on the leg. A serious game was used to motivate the user participation in the test how is shown in Fig 1.

Fig. 2 shows control results obtained when a healthy user is testing the platform. The compliance control is configured with a virtual stiffness $K_v = 20\ N \cdot m/rad$ and $\varepsilon = 0.03$.

The platform movement reference ϕ_l^d is defined as a square signal, with an amplitude of $0.2\ rad$ and period of $24\ s$. The reference signal of the serious game ϕ_l^g is a box that appears and disappears in the center of the screen at each $6\ s$. That is, it appears at the middle time of the upper and lower values of the platform reference signal and disappears when the reference changes its value. Also, on the screen, there is a ball that represents the foot position.

When the box disappears, e.g., the range of time between 0 to $6\ s$, the user is asked for do not apply force to the platform. Within of this range of time the muscular activity is low, thus, the controller remains in the passive mode, $\theta_k = 2$, and the platform is carrying the foot. Notice that, the platform torque is tracking the desired torque. When the box appears, e.g. the range of time between 6 to 12 s, the user is asked to put the ball in the center of the box. The visual feedback causes a human torque opposite to the platform torque, so the muscular activity is high, and the control remains in the resistive mode, $\theta_k = 1$. Likewise, the platform torque is tracking the desired torque. The test had a duration of 42 s, and the stability of the system can be verified.

VI. Results

We calculate the actual stiffness of the system to quantifier the accuracy of the compliance control. From (3), the desired torque is expressed as $\tau_d = K_v e_\phi$, where $e_\phi = \phi_l^d - \phi_l + \varepsilon\dot{\phi}_l^d$. The actual stiffness of the system, K_r, is obtained from root mean square values of the platform torque and position error, thus, $K_r = RMS_{\tau_{plat}}/RMS_{e_\phi}$. The error between the virtual stiffness and the actual stiffness is calculated from $e_{K_v} = |(K_v - K_r)/K_v| \cdot 100\%$. Finally, the results of the accuracy of compliance control for the test shown in Fig. 2 are $K_r = 20.31\ N \cdot m/rad$ and $e_{K_v} = 1.57\%$.

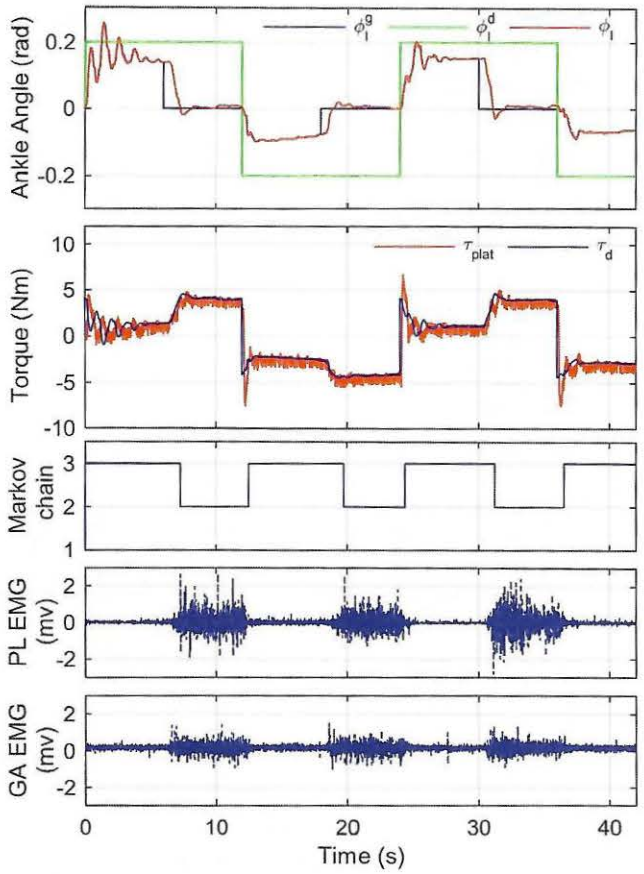

Fig. 2. **Markovian compliance control response based on electromyographic signals:** From the top of figure, we can see the angular ankle position, ϕ_l (red), the platform movement reference, ϕ_l^d (green), and the reference signal of the serious game, ϕ_l^g (blue); the desired torque, τ_d, in blue and platform torque, $\tau_{plat} = \mathcal{J}F_s$, in red; the Markov chain and electromyographic signals from Peroneus Longus (PL) and Gastrocnemius (GA) muscles, respectively.

VII. Conclusions

In this paper, we dealt with the design of a compliance control based on RKF and RR-DMJLS. It incorporates ankle joint impedance in the nominal model. Experimental results obtained from a healthy user using the SRPAR and playing a serious game showed accuracy in the compliance control of 98.43%. The use of electromyographic signals of Peroneus Longus and Gastrocnemius allowed detecting the jump parameter that relates the neuromuscular system with the robotic platform control behavior.

Appendix
Design Parameters

Equations (24) and (25) show matrices that represent each operation mode of the system (17), according with the human parameters defined in Table I. The uncertainty

matrices $H_{i,k}$, $E_{F_{i,k}}$, and $E_{B_{i,k}}$ were computed based on [7]. The parameters tuned for the RKF and RR-DMJLS are shown in Table II.

$$\underbrace{\begin{bmatrix} 0.799 & -12.28 & 0 & 0 \\ 0.002 & 0.987 & 0 & 0 \\ 0 & 0 & 1 & 0 \\ 0 & -0.002 & 0 & 1 \end{bmatrix}}_{F_{1,K}}, \underbrace{\begin{bmatrix} 11.96 \\ 0.012 \\ 0 \\ 0 \end{bmatrix}}_{B_{1,k}}, \underbrace{\begin{bmatrix} 212 & 281 \\ 0.22 & 0.29 \\ 0 & 0 \\ 0 & 0 \end{bmatrix}}_{G_{1,k}},$$

$$\underbrace{\begin{bmatrix} -0.0594 \\ -0.0005 \\ 5 \\ 0.0005 \end{bmatrix}}_{H_{1,k}}, \quad \begin{aligned} E_{F_{1,k}} &= \begin{bmatrix} -0.6 & -496 & 129 & 4804 \end{bmatrix}, \\ E_{B_{1,k}} &= \begin{bmatrix} -59.3 \end{bmatrix}, \\ E_{G_{1,k}} &= \begin{bmatrix} -59300 & -59300 \end{bmatrix}. \end{aligned} \tag{24}$$

$$\underbrace{\begin{bmatrix} 0.663 & -25.24 & 0 & 0 \\ 0.002 & 0.973 & 0 & 0 \\ 0 & 0 & 1 & 0 \\ 0 & -0.002 & 0 & 1 \end{bmatrix}}_{F_{2,K}}, \underbrace{\begin{bmatrix} 19.73 \\ 0.021 \\ 0 \\ 0 \end{bmatrix}}_{B_{2,k}}, \underbrace{\begin{bmatrix} 743 & 98.6 \\ 0.794 & 0.11 \\ 0 & 0 \\ 0 & 0 \end{bmatrix}}_{G_{2,k}},$$

$$\begin{aligned} E_{F_{2,k}} &= \begin{bmatrix} -4 & -477 & 1824 & 6673 \end{bmatrix}, \\ E_{B_{2,k}} &= \begin{bmatrix} -142 \end{bmatrix}, H_{2,k} = H_{1,k}, \\ E_{G_{2,k}} &= \begin{bmatrix} -47460 & -47460 \end{bmatrix}. \end{aligned} \tag{25}$$

TABLE II
DESIGN PARAMETERS

Robust Regulator for DMJLS	
$R_{c,1,k} = R_{c,2,k} = 1$	$\lambda_{c,i,k} = 1 \cdot 10^{17}$
$Q_{c,1,k} = Q_{c,2,k} = I_4$	$\mu_c = 3.99 \cdot 10^{15}$
$P_{c,1}(N) = I_4 \cdot 10^{10}$	$P_{c,1}(N) = P_{c,2}(N)$
Robust Kalman Filter for DMJLS	
$\mu = 1 \cdot 10^{10}$, $\alpha = 2$	$\bar{F}_{i,k} = F_{i,k}(1:2, 1:2)$
$\bar{B}_{i,k} = B_{i,k}(1:2)$	$\bar{G}_{i,k} = G_{i,k}(1:2, 1:2)$
$\bar{C}_{i,k} = [0 \;\; 1]$, $\bar{D}_{i,k} = 1$	$R_k = 0.1$, $Q_k = I_2$
$P_1(N) = I_2 \cdot 10^{15}$	$P_1(N) = P_2(N)$
$E_{\bar{F}_{i,k}} = E_{F_{i,k}}(1, 1:2)$	$E_{\bar{B}_{i,k}} = E_{B_{i,k}}$
$M_{i,k} = H_{2,k}(1:2)$	

REFERENCES

[1] P. S. Lum, C. G. Burgar, P. C. Shor, M. Majmundar, and M. V. der Loos, "Robot-assisted movement training compared with conventional therapy techniques for the rehabilitation of upper-limb motor function after stroke," *Archives of Physical Medicine and Rehabilitation*, vol. 83, no. 7, pp. 952 – 959, 2002.

[2] L. Marchal-Crespo and D. J. Reinkensmeyer, "Review of control strategies for robotic movement training after neurologic injury," *Journal of neuroengineering and rehabilitation*, vol. 6, no. 1, p. 20, 2009.

[3] P. K. Jamwal, S. Hussain, and S. Q. Xie, "Review on design and control aspects of ankle rehabilitation robots," *Disability and Rehabilitation: Assistive Technology*, vol. 10, no. 2, pp. 93–101, 2015.

[4] T. B. Sheridan, "Human–robot interaction: status and challenges," *Human factors*, vol. 58, no. 4, pp. 525–532, June 2016.

[5] X. Li, Y. Pan, G. Chen, and H. Yu, "Adaptive human-robot interaction control for robots driven by series elastic actuators," *IEEE Transactions on Robotics*, vol. 33, no. 1, pp. 169–182, February 2017.

[6] M. Semprini, A. V. Cuppone, I. Delis, V. Squeri, S. Panzeri, and J. Konczak, "Biofeedback signals for robotic rehabilitation: Assessment of wrist muscle activation patterns in healthy humans," *IEEE Transactions on Neural Systems and Rehabilitation Engineering*, vol. 25, no. 7, pp. 883–892, July 2017.

[7] A. L. Jutinico, J. C. Jaimes, F. M. Escalante, J. C. Perez-Ibarra, M. H. Terra, and A. A. G. Siqueira, "Impedance control for robotic rehabilitation: A robust markovian approach," *Frontiers in Neurorobotics*, vol. 11, p. 43, August 2017.

[8] A. L. Jutinico, J. C. Jaimes, F. M. Escalante, J. C. Perez-Ibarra, M. H. Terra, and A. A. Siqueira, "Recursive robust regulator for discrete-time markovian jump linear systems: Control of series elastic actuators," *IFAC-PapersOnLine*, vol. 50, no. 1, pp. 1340 – 1345, 2017, 20th IFAC World Congress.

[9] J. P. Cerri, "Controle e filtragem para sistemas lineares discretos incertos sujeitos a saltos markovianos," Ph.D. dissertation, Escola de Engenharia de São Carlos, Universidade de São Paulo, 2013.

[10] J. Y. Ishihara, M. H. Terra, and J. P. Cerri, "Optimal robust filtering for systems subject to uncertainties," *Automatica*, vol. 52, pp. 111 – 117, 2015.

[11] J. P. Cerri and M. H. Terra, "Recursive robust regulator for discrete-time markovian jump linear systems," *IEEE Transactions on Automatic Control*, vol. 62, no. 11, pp. 6004–6011, November 2017.

[12] F. M. Escalante, A. L. Jutinico, J. C. Jaimes, A. A. G. Siqueira, and M. H. Terra, "Robust kalman filter and robust regulator for discrete-time markovian jump linear systems: Control of series elastic actuator," in *2018 Conference on Control Technology and Applications (CCTA). (Accepted to present)*, August 2018.

[13] D. W. Robinson, J. E. Pratt, D. J. Paluska, and G. A. Pratt, "Series elastic actuator development for a biomimetic walking robot," in *1999 IEEE/ASME International Conference on Advanced Intelligent Mechatronics (Cat. No.99TH8399)*, September 1999, pp. 561–568.

[14] H. Lee, E. J. Rouse, and H. I. Krebs, "Summary of human ankle mechanical impedance during walking," *IEEE Journal of Translational Engineering in Health and Medicine*, vol. 4, pp. 1–7, August 2016.